Available online at www.sciencedirect.com
SCIENCE DIRECT®

Journal of Sound and Vibration 266 (2003) 967–980

JOURNAL OF SOUND AND VIBRATION

www.elsevier.com/locate/jsvi

Acoustic characteristics of annular cavities with locally non-uniform media

Hyoung Gil Choi[a,*], Sung Woo Yoo[b], Ji Deok Jeong[c], Jang Moo Lee[c]

[a] *Turbo and Power Machinery Research Center, Seoul National University, San 56-1, Shillim-dong, Kwanak-gu, Seoul 151-742, South Korea*

[b] *ArvinMeritor Technical Center, 950 W 450 S, Columbus, IN 47201, USA*

[c] *School of Mechanical and Aerospace Engineering, Seoul National University, San 56-1, Shillim-dong, Kwanak-gu, Seoul 151-742, South Korea*

Received 21 February 2002; accepted 1 October 2002

Abstract

A theoretical approach is developed to obtain the natural frequencies and the mode shapes of annular cavities that have locally non-uniform media. The equation of motion is derived based on a special form of the wave equation that is capable of representing the variation of material properties with position, and the unit step function is used in the equation to express the local non-uniformity of the media. The Laplace transform is adopted in eigenvalue analysis to calculate the natural frequencies and the normal mode shapes of the annular cavities. The validity of the presented method is verified through finite element analysis and experiments. Parametric studies are performed to find out the relation between the acoustic characteristics of the cavity and the local deviation of the media, and the acoustic characteristics are explained in terms of the mass and stiffness effect of the local deviation in an annular cavity upon the natural vibration characteristics.

1. Introduction

The vibration or acoustic problems of cylinder-shaped machines are frequently caused by the resonance in the interior cylindrical cavities. Generally, the cylindrical cavities in the machines are not perfectly axisymmetric but locally asymmetric, or have non-uniform distribution of medium, making these problems difficult to analyze.

*Corresponding author. Tel.: +82-2-880-7152; fax: +82-2-876-9493.

E-mail addresses: hgchoi@vib.snu.ac.kr (H.G. Choi), Sung-Woo.Yoo@ArvinMeritor.com (S.W. Yoo), jjd@vib.snu.ac.kr (J.D. Jeong), leejm@gong.snu.ac.kr (J.M. Lee).

doi:10.1016/S0022-460X(02)01383-4

Acoustic problems of this type are similar to vibration problems of membranes and many studies have been made mainly in inhomogeneous membranes. Gottlieb [1] investigated the vibrations of rectangular stepped-density membranes and the relationship between the density ratio and the natural frequency. Cortinez and Laura [2] also studied the vibrations of rectangular membranes by using the Kantorovich method and compared eigenvalues in variation of density ratio, non-homogeneous area ratio and aspect ratio of a rectangular membrane. The free vibrations of a rectangular membrane with unidirectional and smoothly varying inhomogeneity were investigated by means of the approximate analytical method [3] and the optimized Galerkin–Kantorovich and the differential quadrature method [4]. Also, the analyses of circular and annular membranes with non-uniform radial density were made in the Refs. [5–7]. In Ref. [5], the method of constant density radial segments was used, and especially in the papers by Gutierrez et al. [6] and Bala Subrahmanyam et al. [7], the axisymmetric vibrations of annular membranes with linearly, quadratically, and cubically varying radial density were analyzed and the effect of the density variation to eigenvalues were investigated.

Moreover, asymmetrical structures, such as a ring or a shell with slight local deviation, have been analyzed. Hong and Lee [8] obtained an exact solution of circular rings with a small local deviation using a new method, without any trial functions for mode shapes and the use of finite elements. Chung and Lee [9] developed a new conical ring element used in connection with FEM in order to consider the effects of slight local deviations from an axisymmetric ring, and analyzed the free vibrations of a nearly axisymmetric shell structure such as a Korean bell, using this element.

In electromagnetic theory, problems of this type are of deep interest. In Ref. [10], electromagnetic fields in structures composed of inhomogeneous cylindrical layers were analyzed using a propagator matrix approach. In Ref. [11], the finite-difference method was used to make the full-wave analysis of the generalized microstrip line on an inhomogeneous anisotropic substrate.

In this paper, an analytical study is made to investigate the natural frequencies and mode shapes of acoustic cavities with locally non-uniform media. The exact solution of the annular cavities with the media deviation only in the circumferential direction is obtained using the Laplace transform of the eigenvalue problem and the radial dependence is disregarded. The validity of this approach is examined through finite element analysis and experiments. Based on the solution, the effects of local variations of acoustic properties to global modal characteristics were evaluated through several simulations. The presented analysis can be applied to the structural-acoustic coupling problems of annular ducts.

2. Theoretical formulation

The wave equation of an acoustic cavity with local deviation in media is given as [12,13]

$$\nabla \cdot \left(\frac{1}{\rho_0} \nabla p \right) - \frac{1}{B_0} \frac{\partial^2 p}{\partial t^2} = 0, \tag{1}$$

where p denotes the acoustic pressure in the cavity, and c_0, ρ_0 and B_0 are the speed of sound, density, and bulk modulus of the medium, respectively. If the acoustic variation in the axial

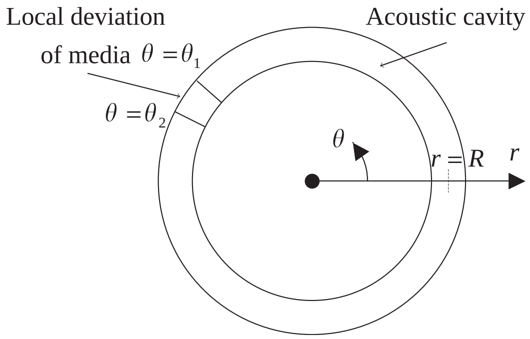

Fig. 1. An annular cavity with local deviation of medium.

direction of the cylinder is ignored, the dual cylinder model can be simplified to the two-dimensional annular model as shown in Fig. 1. If it is assumed that the width of the annular cavity is sufficiently small in comparison with its radius, the acoustic variation in the radial direction is ignored and only that in the circumferential direction is considered.[1]

When the properties of the medium in $\theta_1 \leqslant \theta \leqslant \theta_2$ are different from those of the other part as shown in Fig. 1, the density, speed of sound, and bulk modulus are represented as follows:

$$\begin{aligned} \rho_0 &= \rho_u + \rho_a\{\mathrm{H}(\theta - \theta_1) - \mathrm{H}(\theta - \theta_2)\}, \\ c_0 &= c_u + c_a\{\mathrm{H}(\theta - \theta_1) - \mathrm{H}(\theta - \theta_2)\}, \\ B_0 &= B_u + B_a\{\mathrm{H}(\theta - \theta_1) - \mathrm{H}(\theta - \theta_2)\}, \end{aligned} \tag{2}$$

where $\mathrm{H}(\cdot)$ is the Heaviside unit step function, and ρ, c and B are the density, speed of sound, and bulk modulus, respectively. The subscript "u" denotes uniform properties of a large part of the medium and "a" denotes added properties of the deviation part. Since the radial variation is ignored, we can represent Eq. (1) as follows:

$$\frac{1}{r^2}\frac{\partial}{\partial\theta}\left(\frac{1}{\rho_0}\right)\frac{\partial p}{\partial\theta} + \frac{1}{r^2\rho_0}\frac{\partial^2 p}{\partial\theta^2} - \frac{1}{B_0}\frac{\partial^2 p}{\partial t^2} = 0. \tag{3}$$

As a matter of convenience, $1/\rho_0$ and $1/B_0$ in Eq. (3) are transposed to Eq. (4)

$$\rho_0^* = \frac{1}{\rho_0} = \frac{1}{\rho_u + \rho_a(\mathrm{H}_1 - \mathrm{H}_2)} = \rho_u^* + \rho_a^*(\mathrm{H}_1 - \mathrm{H}_2),$$

$$B_0^* = \frac{1}{B_0} = \frac{1}{B_u + B_a(\mathrm{H}_1 - \mathrm{H}_2)} = B_u^* + B_a^*(\mathrm{H}_1 - \mathrm{H}_2),$$

[1] Numerical analyses and physical experiments shown in other sections of the paper corroborate this assumption for a certain range of the geometric parameters. The validity of this assumption is shown in the appendix.

$$\rho_u^* = \frac{1}{\rho_u}, \quad \rho_a^* = \frac{1}{\rho_u + \rho_a} - \frac{1}{\rho_u}, \tag{4}$$

$$B_u^* = \frac{1}{B_u}, \quad B_a^* = \frac{1}{B_u + B_a} - \frac{1}{B_u}.$$

If Eq. (4) is substituted into Eq. (3), the equation of motion is

$$\rho_0^* \frac{\partial^2 p}{\partial \theta^2} + \frac{\partial \rho_0^*}{\partial \theta} \frac{\partial p}{\partial \theta} - r^2 B_0^* \frac{\partial^2 p}{\partial t^2} = 0. \tag{5}$$

Assuming $p(\theta, t) = P(\theta)e^{j\omega t}$ and replacing coefficients of Eq. (5) with Eq. (4), the eigenvalue problem is derived as

$$\{\rho_u^* + \rho_a^*(\mathrm{H}_1 - \mathrm{H}_2)\}P'' + \rho_a^*(\delta_1 - \delta_2)P' + r^2\omega^2\{B_u^* + B_a^*(\mathrm{H}_1 - \mathrm{H}_2)\}P = 0, \tag{6}$$

where

$$P' = \mathrm{d}P(\theta)/\mathrm{d}\theta, \quad P'' = \mathrm{d}^2 P(\theta)/\mathrm{d}\theta^2, \quad 0 \leqslant \theta \leqslant 2\pi, \quad 0 \leqslant \theta_1 \leqslant \theta_2 \leqslant 2\pi,$$
$$\mathrm{H}_i = \mathrm{H}(\theta - \theta_i), \quad \delta_i = \delta(\theta - \theta_i) \quad (i = 1, 2).$$

Eq. (6) is the governing equation of motion for an annular cavity with a local deviation of media. Matching boundary conditions, that is, continuity conditions of acoustic pressure and velocity at the arbitrary position are represented as

$$P(\theta) = P(\theta + 2\pi), \quad V(\theta) = V(\theta + 2\pi). \tag{7}$$

Also, the pressure and velocity should be continuous at $\theta = \theta_1$. If we denote θ_1^+ and θ_1^- as the limits of $\theta_1 + \varepsilon$ and $\theta_1 - \varepsilon$ as ε approaches zero, the continuity conditions

$$P(\theta_1^+) = P(\theta_1^-), \quad P'(\theta_1^+) = \frac{\rho_u + \rho_a}{\rho_u} P'(\theta_1^-) \tag{8}$$

must be satisfied, and the continuity conditions at $\theta = \theta_2$ are analogous.

Substituting continuity conditions (7) and (8) into Eq. (6), the Laplace transform [14] of Eq. (6) is as follows:

$$(s^2 + Z^2)\bar{P}(s) = sP(0) + P'(0) + \{s\rho_r \hat{P}'(\theta_0) + Z^2 B_r \hat{P}(\theta_0)\}e^{-s\theta_0}, \tag{9}$$

where

$$Z = r\omega/c_u, \quad \rho_r = \rho_a\,\Delta\theta/\rho_u, \quad B_r = B_a\,\Delta\theta/(B_u + B_a),$$

$$\hat{P}^{(n)}(\theta_0) = \frac{P^{(n)}(\theta_1^-) + P^{(n)}(\theta_2^+)}{2} \quad (n = 0, 1). \tag{10}$$

Using the inverse Laplace transform, we obtain the following equation:

$$P(\theta) = A\cos Z\theta + B\sin Z\theta + \mathrm{H}(\theta-\theta_0)\{C\cos[Z(\theta-\theta_0)] + D\sin[Z(\theta-\theta_0)]\}, \tag{11}$$

where

$$A = P(0),\ B = P'(0)/Z,\ C = \rho_r\hat{P}'(\theta_0),\ D = B_r Z\hat{P}(\theta_0). \tag{12}$$

If we apply the matching boundary conditions (7) to Eq. (11), the result is

$$\begin{bmatrix} \cos(2\pi Z)-1 & \sin(2\pi Z) \\ -\sin(2\pi Z) & \cos(2\pi Z)-1 \end{bmatrix}\begin{pmatrix} A \\ B \end{pmatrix} = -\begin{bmatrix} \cos[Z(2\pi-\theta_0)] & \sin[Z(2\pi-\theta_0)] \\ -\sin[Z(2\pi-\theta_0)] & \cos[Z(2\pi-\theta_0)] \end{bmatrix}\begin{pmatrix} C \\ D \end{pmatrix}. \tag{13}$$

From Eq. (13), two forms of the solutions are considered. First, when the determinant of the 2×2 matrix of the left side is zero, Z is an integer. In this case, C and D become zero, so that

$$P(\theta) = A_s\sin[n(\theta-\phi_s)], \tag{14}$$

where A_s and ϕ_s are constants. If $\rho_r \neq 0$, then $\hat{P}(\theta_0) = \hat{P}'(\theta_0) = 0$; therefore only the trivial solution will be obtained. If $\rho_r = 0$ and $B_r \neq 0$, then $\hat{P}(\theta_0) = 0$; therefore the solution of $P(\theta) = A_s\sin[n(\theta-\theta_0)]$ is obtained. The second case is when the determinant is not zero, that is, Z is not an integer. In this case, A and B in Eq. (13) can be expressed as functions of C and D. Then from Eq. (11), we obtain

$$\begin{aligned} P(\theta) = &-\frac{\sin[Z(\theta-\theta_0+\pi)]}{2\sin(\pi Z)}C + \frac{\cos[Z(\theta-\theta_0+\pi)]}{2\sin(\pi Z)}D \\ &+ H(\theta-\theta_0)\{C\cos[Z(\theta-\theta_0)] + D\sin[Z(\theta-\theta_0)]\}. \end{aligned} \tag{15}$$

Using pressure equation (15), $\hat{P}(\theta_0)$ and $\hat{P}'(\theta_0)$ defined in Eq. (10) are obtained as follows:

$$\hat{P}(\theta_0) = \frac{D\cos[Z(\pi-\Delta\theta/2)]}{2\sin(\pi Z)},\quad \hat{P}'(\theta_0) = -\frac{CZ\cos[Z(\pi-\Delta\theta/2)]}{2\sin(\pi Z)}. \tag{16}$$

If C and D in Eq. (12) are substituted in Eq. (16), we obtain the final equation of this problem

$$\begin{bmatrix} p(Z)-1 & 0 \\ 0 & q(Z)-1 \end{bmatrix}\begin{pmatrix} \hat{P}(\theta_0) \\ \hat{P}'(\theta_0) \end{pmatrix} = \begin{pmatrix} 0 \\ 0 \end{pmatrix}, \tag{17}$$

where

$$p(Z) = \frac{B_r Z\cos[Z(\pi-\Delta\theta/2)]}{2\sin(\pi Z)},\quad q(Z) = -\frac{\rho_r Z\cos[Z(\pi-\Delta\theta/2)]}{2\sin(\pi Z)}. \tag{18}$$

If $\hat{P}(\theta) = \hat{P}'(\theta) = 0$, then Eq. (17) has the trivial solution. Therefore in order to obtain the non-trivial solution, the following equation must be satisfied:

$$\{p(Z)-1\}\{q(Z)-1\} = 0. \tag{19}$$

First, when $p(Z) - 1 = 0$, the natural frequencies can be obtained from Z's that are the roots of this equation, and the normal mode shapes result in the following forms:

$$P(\theta) = \left\{ \frac{\cos[Z(\theta - \theta_0 + \pi)]}{2\sin(\pi Z)} + \mathrm{H}(\theta - \theta_0)\sin[Z(\theta - \theta_0)] \right\} D. \tag{20}$$

Next when $q(Z) - 1 = 0$, the normal mode shapes are

$$P(\theta) = \left\{ -\frac{\sin[Z(\theta - \theta_0 + \pi)]}{2\sin(\pi Z)} + \mathrm{H}(\theta - \theta_0)\cos[Z(\theta - \theta_0)] \right\} C. \tag{21}$$

With respect to the diameter passing through the local deviation at θ_0, Eq. (20) represents symmetric modes and Eq. (21) asymmetric modes. Only if $\rho_r = 0$, the asymmetric modes are

$$P(\theta) = A_s \sin[n(\theta - \theta_0)]. \tag{22}$$

3. Verification

The proposed method was validated by comparing the natural frequencies and mode shapes obtained from this method to the results from FEA and modal test. Mass and stiffness effects of local deviation upon system characteristics were verified by FEA, and the combined effect was also verified by modal test for an actual cavity.

3.1. Verification of the mass and the stiffness effects

An annular cavity with the geometry and properties shown in Table 1 was analyzed to verify the mass and stiffness effects of the local deviation. In FEA, the cavity was modelled by 7920 nodes and 7200 elements. The position of deviation was 90°, and its size was 3°.

To verify the mass effect, a cavity with the density deviation of 10 times bigger than the other part was analyzed by the proposed method and a commercial FEA program (SYSNOISE). The results from the two methods agree with each other very well as shown in Table 2 and Fig. 2.

A cavity with the sound-speed deviation of 10 times bigger than the other part was also used to verify the stiffness effect. The results are compared in Table 3 and Fig. 3. It is found that the results from the proposed method agree well with the FEA results.

Table 1
Geometry and acoustic properties of an annular cavity with locally non-uniform medium for verification of the proposed method

Geometry	Radius	1 m
	Position of local deviation	90°
	Size of local deviation	3°
Property	Ambient	1.21 kg/m^3, 340 m/s
	Density variation ($\times$ 10)	12.10 kg/m^3, 340 m/s
	Sound-speed variation ($\times$ 10)	1.21 kg/m^3, 3400 m/s

Table 2
Natural frequencies of the annular cavity with local density deviation of medium

Mode	FEM (Hz)	Proposed method (Hz)	Difference (%)[a]
1-1	50.433	50.411	−0.044
1-2	54.545	54.522	−0.042
2-1	101.263	101.217	−0.045
2-2	109.090	109.043	−0.043
3-1	152.705	152.632	−0.048
3-2	163.636	163.566	−0.043

[a] Difference (%) = {(proposed method)−(FEM)}/(FEM) × 100.

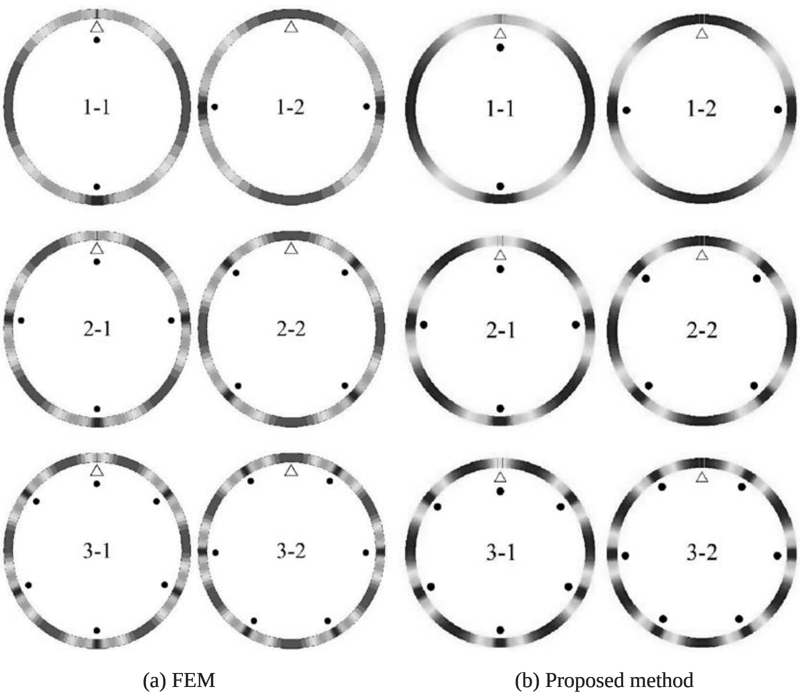

Fig. 2. Normal mode shapes of the annular cavity with local density deviation of medium (△: deviation position, ●: nodal point).

As shown in Figs. 2 and 3, the center point of the deviation area is an anti-nodal point for symmetric modes, but a nodal point for unsymmetrical modes.

3.2. Verification in the case of a real physical system

The experimental setup of a real system is shown in Fig. 4. Geometries of the acryl cavity and experimental equipments are summarized in Table 4. The material used in the deviation is a type

Table 3
Natural frequencies of the annular cavity with local stiffness deviation of medium

Mode	FEM (Hz)	Proposed method (Hz)	Difference (%)[a]
1-1	54.136	54.113	−0.042
1-2	54.586	54.563	−0.042
2-1	108.273	108.225	−0.044
2-2	109.173	109.126	−0.043
3-1	162.412	162.338	−0.046
3-2	163.760	163.690	−0.043

[a] Difference (%) = {(proposed method)−(FEM)}/(FEM) × 100.

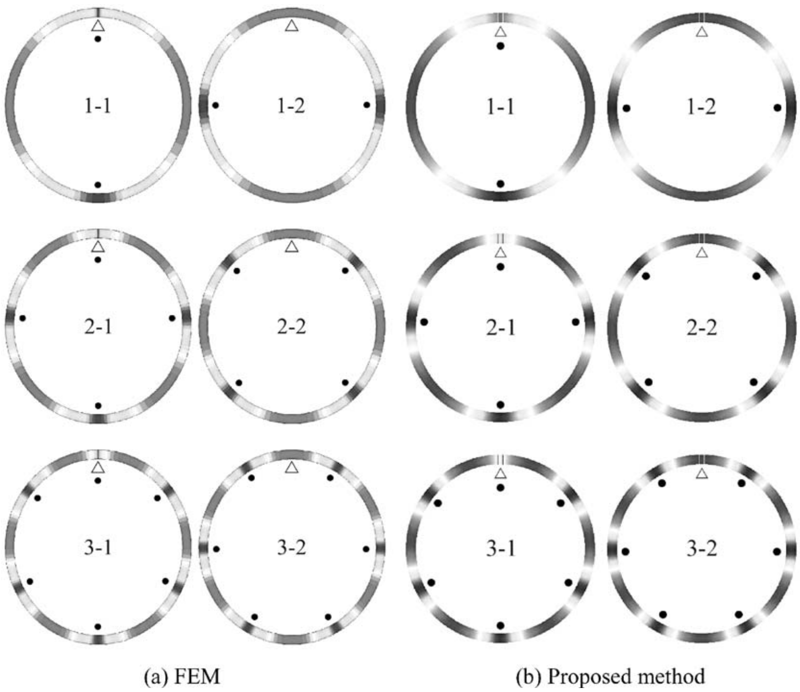

Fig. 3. Normal mode shapes of the annular cavity with local stiffness deviation of medium (△: deviation position, ●: nodal point).

of cream, and its density and speed of sound are 266 kg/m^3 and 440 m/s, respectively. The density is measured as the mass per unit volume, and the speed of sound is calculated from the results of the transmission loss measurements. The length of the deviation is 17 mm.

The results obtained by the analysis and the experiment are shown in Table 5. The equivalent radius used in the analyses is 270 mm and the equivalent size of the deviation is 3.6°. As shown in Table 5, the two results are very close within 1% error, therefore the proposed method is verified as a method suitable to demonstrate the effects of the deviation.

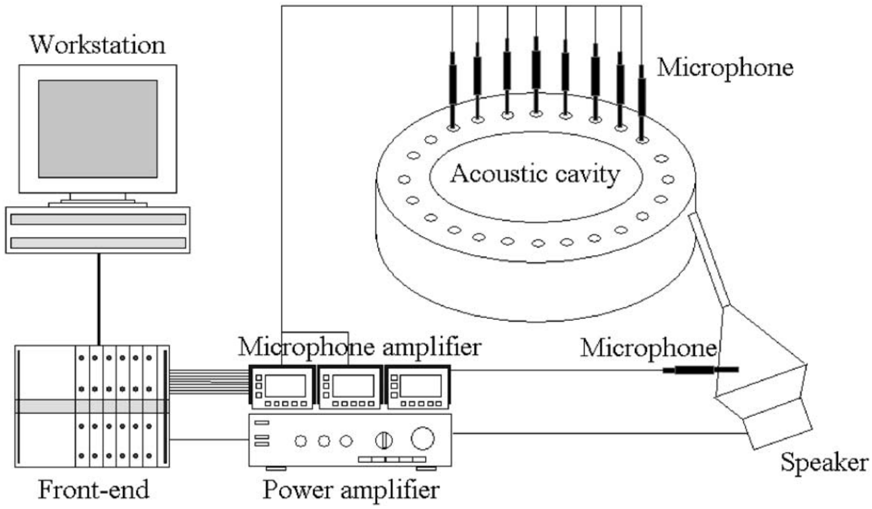

Fig. 4. Schematic diagram of the experimental setup for verification of the application of the proposed method to real systems.

Table 4
Geometry of a cavity and experimental equipments for acoustic modal test

Geometry	Acoustic cavity	Inner diameter	500 mm
		Outer diameter	580 mm
		Height	153 mm
	Acryl structure	Panel thickness	15 mm
		Cylinder thickness	10 mm
		Outer diameter	500 mm
		Outer diameter	600 mm
Equipment	Microphone	Bruel & Kjaer type 4196	
	Speaker	Diameter 6 inch	
	Microphone amplifier	NEXUS conditioning amplifier 2690A0S4	
	Speaker power amplifier	Inkel stereo integrated amplifier AX7030R	
	Front-end	SCADAS II SG206-B	
	Modal software	LMS/CADA-X ver3.4	

4. Parametric studies

To illustrate the effects of the density and sound-speed variation in the deviation on the acoustic characteristics of cavities, parametric studies are conducted. The position of the deviation is 90°, and its size is 3°. Changes of natural frequencies and mode shapes according to the variation of density and sound speed are investigated for the first and second mode pairs.

Table 5
Natural frequencies of the experimental annular cavity with locally non-uniform medium from test and proposed analysis

Mode	Proposed method (Hz)	Experiment (Hz)	Difference (%)[a]
1-1 (1,0)	116.898	117.618	−0.612
1-2 (2,0)	202.436	204.407	−0.964
2-1 (3,0)	309.677	311.696	−0.648
2-2 (4,0)	404.875	407.332	−0.603
3-1 (5,0)	509.757	513.981	−0.822
3-2 (6,0)	607.318	606.786	+0.088

[a] Difference (%) = {(proposed method)−(experiment)}/(experiment) × 100.

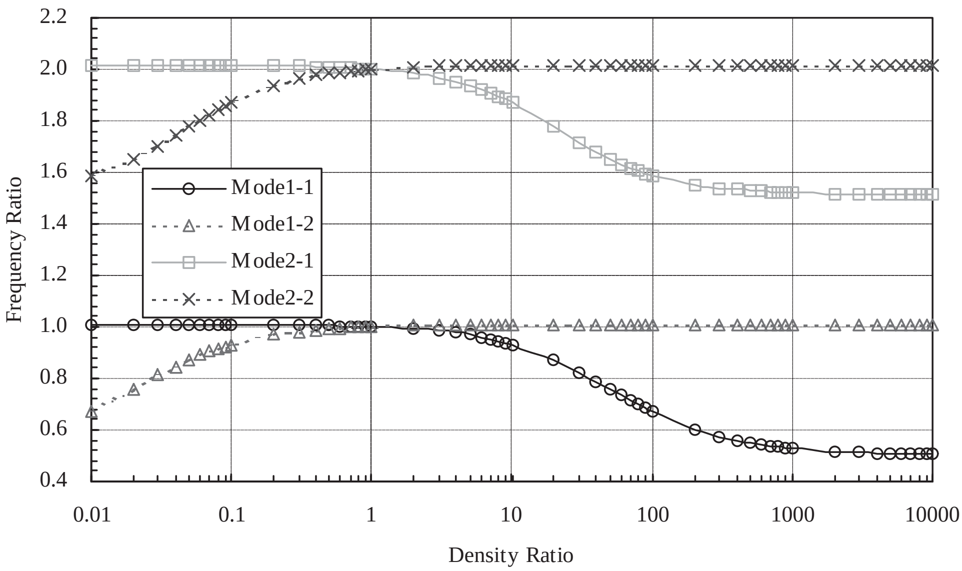

Fig. 5. Natural frequency ratios with variations of the density in deviation.

4.1. Modal changes due to the mass variation

Natural frequency change according to the variation of density in deviation is shown in Fig. 5, and mode shapes are plotted in Fig. 6. In the figures, the natural frequency ratio is defined as the ratio of the natural frequency of the cavity with deviation to the first natural frequency of that without deviation, and the density ratio as a ratio of the density in deviation to the ambient density.

When density ratio decreases to less than 1, (2,0) and (4,0) symmetric modes—an anti-nodal point is located in the deviation—are changed similarly to (1,0) and (3,0) modes, respectively, but anti-symmetric modes—a nodal point is located in the deviation—do not change. To the contrary,

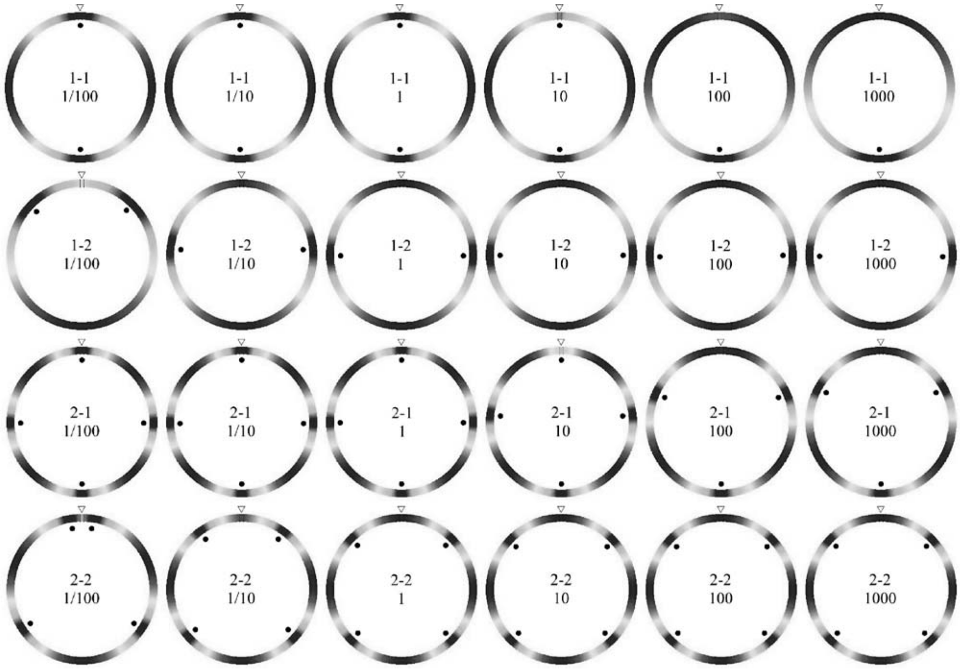

Fig. 6. Normal mode shapes with variations of the density in deviation (∇: deviation position, ●: nodal point).

when density ratio increases to greater than 1, $(2n, 0)$ anti-symmetric modes are changed to $(2n-1, 0)$ modes, but symmetric modes do not change. In other words, an anti-node at deviation changes to a node as density ratio decreases, and a node at deviation changes to an anti-node as density ratio increases.

4.2. Modal changes due to the stiffness variation

Natural frequency changes according to the variation of sound speed in deviation are shown in Fig. 7, and the mode shapes are plotted in Fig. 8. Unlike the mass effect, when the sound-speed ratio only decreases, $(2n,\ 0)$ symmetric modes change similarly to $(2n-1,\ 0)$ modes, but modes do not change in the other case. Therefore the decrease makes the deviation an open boundary.

5. Conclusions

In this study, we investigated an analytical method to illustrate natural frequencies and mode shapes of acoustic cavities with a local deviation. Based on the wave equation that can represent the local deviation in media, the Laplace transform was used to obtain an exact solution. Local deviations were mathematically modelled using the Heaviside step function.

For an annular cavity with a local deviation of media, the theoretical analysis, FEA and experiments were conducted and the theoretical analysis was verified by comparing their results.

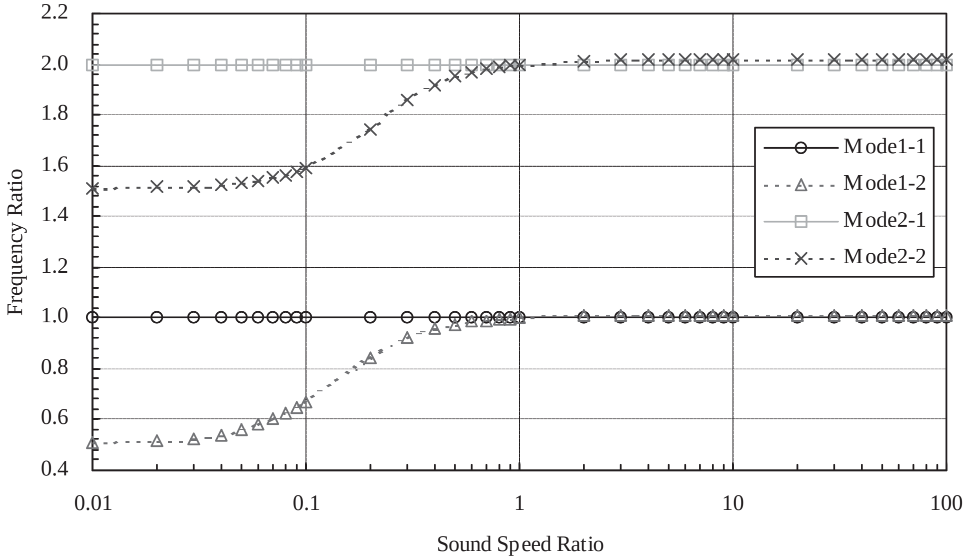

Fig. 7. Natural frequency ratios with variations of the sound speed in deviation.

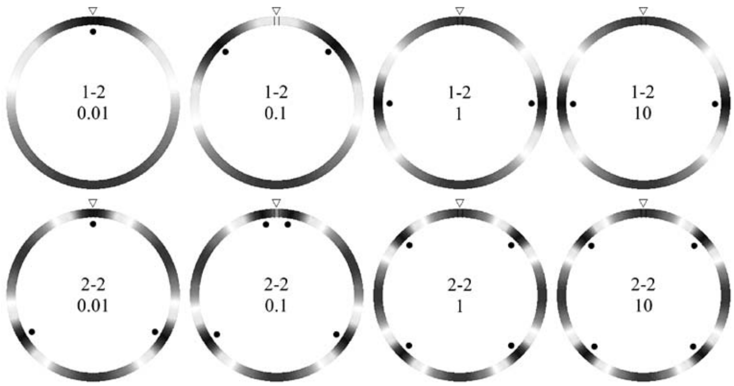

Fig. 8. Normal mode shapes with variations of the sound speed in deviation (▽: deviation position, ●: nodal point).

From parametric studies, we investigated the effects of the density and sound speed in deviation on acoustic characteristics—natural frequencies and symmetric/anti-symmetric mode shapes of cavities.

Acknowledgements

This work was supported by the Brain Korea 21 Project, Mechanical Engineering Research Division.

Table 6
Comparison of eigenvalues of an annular cavity obtained analytically and by FEA

w/r[a]	(2,0) mode (Hz)		Error (%)[b]	
	Analytical	FEA	Analytical	FEA
0.1	54.135	54.137	0.042	0.045
0.2	54.202	54.204	0.165	0.169
0.3	54.311	54.313	0.366	0.369
0.4	54.457	54.459	0.636	0.640
0.5	54.635	54.638	0.966	0.970
0.6	54.837	54.839	1.339	1.343
0.7	55.050	55.052	1.732	1.717
0.8	55.260	55.262	2.120	2.124
0.9	55.447	55.449	2.465	2.469
1.0	55.587	55.589	2.724	2.729

[a] w/r = width/radius.
[b] Reference for error estimation is 54.113 Hz obtained using this assumption.

Appendix A

To verify the validity of this assumption, eigenvalues of an annular cavity are obtained analytically and by FE and varying a geometric parameter, that is, a ratio of its width to its radius from 10% to 100% with an interval of 10%. The neutral radius of the annular cavity is 1 m, and the density and the speed of sound are 1.21 kg/m^3 and 340m/s, respectively. The simulation results are shown in Table 6. From the results, it can be seen that when the ratio of the width to the radius is in the range of less than about 40%, the acoustic variation in the radial direction can be ignored and only that in the circumferential direction is considered.

Appendix B. Nomenclature

p	acoustic pressure
ρ	density
c	speed of sound
B	bulk modulus
t	time
$r,\ \theta$	polar co-ordinates
H_i	Heaviside step function of $\mathrm{H}(\theta - \theta_i)$
δ_i	delta function of $\delta(\theta - \theta_i)$
θ_1, θ_2	starting and ending position angle of the deviation of media, respectively
$\Delta\theta$	angle of the deviation of media
R	radius of the centerline of the annular cavity

References

[1] H.P.W. Gottlieb, New types of vibration modes for stepped membranes, Journal of Sound and Vibration 110 (3) (1986) 395–411.

[2] V.H. Cortinez, P.A.A. Laura, Vibration of non-homogeneous rectangular membranes, Journal of Sound and Vibration 156 (2) (1992) 217–225.

[3] J.A. Masad, Free vibration of a non-homogeneous rectangular membrane, Journal of Sound and Vibration 195 (4) (1996) 675–678.

[4] P.A.A. Laura, R.E. Rossi, R.H. Gutierrez, The fundamental frequency of non-homogeneous rectangular membranes, Journal of Sound and Vibration 204 (2) (1997) 373–376.

[5] T.M. Kalotas, A.R. Lee, The modes of a circular membrane of non-uniform radial density, Acoustica 78 (1993) 220–225.

[6] R.H. Gutierrez, P.A.A. Laura, V. Bambill, V.A. Jederlinic, D.H. Hodges, Axisymmetric vibrations of solid circular and annular membranes with continuously varying density, Journal of Sound and Vibration 212 (4) (1998) 611–622.

[7] P. Bala Subrahmanyam, R.I. Sujith, Exact solutions for axisymmetric vibrations of solid circular and annular membranes with continuously varying density, Journal of Sound and Vibration 248 (2) (2001) 371–378.

[8] J.S. Hong, J.M. Lee, Vibration of circular rings with local deviation, Journal of Applied Mechanics 61 (1994) 317–322.

[9] J. Chung, J.M. Lee, Vibration analysis of a nearly axisymmetric shell structure using a new finite ring element, Journal of Sound and Vibration 219 (1) (1999) 35–50.

[10] B. Jakoby, D. De Zutter, Analysis of guided waves in inhomogeneous bianisotropic cylindrical waveguides, IEEE Transactions on Microwave Theory and Techniques 44 (2) (1996) 297–310.

[11] K. Radhakrishnan, W.C. Chew, Full-wave analysis of multiconductor transmission lines on anisotropic inhomogeneous substrates, IEEE Transactions on Microwave Theory and Techniques 47 (9) (1999) 1764–1770.

[12] A.D. Pierce, Wave equation for sound in fluids with unsteady inhomogeneous flow, Journal of the Acoustical Society of America 87 (6) (1990) 2292–2299.

[13] M.J. Crocker (Editor-in-Chief), Handbook of Acoustics, Wiley, New York, 1998.

[14] M.R. Spiegel, Schaum's Outline of Theory and Problems of Laplace Transforms, McGraw-Hill, Singapore, 1986.